PHYSICAL REVIEW A VOLUME 13, NUMBER 6 JUNE 1976

Temperature dependence of the hydrogen-hydrogen spin-exchange cross section

M. Desaintfuscien and C. Audoin

Laboratoire de l'Horloge Atomique, Equipe de Recherche du Centre National de la Recherche Scientifique, Bât. 221, Université Paris-Sud, 91405 Orsay, France

(Received 12 February 1976)

Spin-exchange relaxation rates are measured, as a function of the atomic hydrogen density, in the storage bulb of a hydrogen maser of special design. The values of the hydrogen-hydrogen spin-exchange cross section in the temperature range 77-363 K result. These experimental values are in very good agreement with the result of a theoretical calculation by Allison. For ambient temperature, the experimental value is $\sigma = 23.1 \pm 2.8$ Å^2 (the theoretical value is 23.5 ± 2.4 Å^2) and it varies slowly with temperature.

The process of electron spin exchange occurring in the collision of two hydrogen atoms in the ground state is of interest in astrophysics,[1-4] atomic physics,[5-10] and in the theory of the hydrogen maser.[8,10]

Theory of the H-H spin-exchange interaction and estimates of the H-H spin-exchange cross section σ have been considered in a number of papers.[1-3,5,7,8,11-15] The most recent and satisfactory calculation of the value of σ has been given by Allison and Dalgarno[16] and Allison,[17] using the precise H-H interaction potential of Kolos and Wolniewicz.[18] Theoretical values of the spin-exchange cross section, averaged over a Maxwellian velocity distribution, are then available for a range of temperature extending from 10 to 1000 K.[17] In contrast, the experimental determinations[7,19-21] of this cross section have all been performed close to room temperature.

In this paper, we report the determination of the hydrogen-hydrogen spin-exchange cross section in the temperature range[22] 77-363 K from measurements made in a hydrogen maser[23,24] of special design.[25]

PRINCIPLE OF MEASUREMENT

In the hydrogen maser, the population difference between the two maser levels as well as the oscillating moment are affected by collisions between hydrogen atoms. We have

$$\gamma_1 = \gamma_{10} + \gamma_{1e} \quad \text{and} \quad \gamma_2 = \gamma_{20} + \gamma_{2e}, \tag{1}$$

where γ_1 and γ_2 are the relaxation rates of the population difference between the two maser levels and of the oscillating moment, respectively; γ_{10} and γ_{20} represent the joint effect of the bulb escape and wall relaxation. γ_{1e} and γ_{2e} characterize the contribution of H-H collisions to the total relaxation rates. They are linked to the total spin-exchange cross section σ by

$$\gamma_{1e} = 2\gamma_{2e} = n\sigma\bar{v}_r, \tag{2}$$

where n is the atomic hydrogen density in the bulb and $\bar{v}_r$ is the mean relative velocity of atoms. The cross section σ is defined as[15]

$$\sigma = \left\langle \frac{\pi}{k^2} \sum_{l=0}^{\infty} (2l+1) \sin^2(\delta_l^1 - \delta_l^3) \right\rangle_k, \tag{3}$$

with $k = \mu v_r / h$, where μ is the reduced mass of the atom, and v_r the relative velocity in a H-H collision. δ_l^1 and δ_l^3 are, respectively, the singlet and triplet scattering phase shifts for partial waves with orbital angular momentum l. The bracket represents the average over a Maxwellian distribution of atomic velocities.

The most direct method for the determination of σ therefore consists in measuring the variation of the relaxation rates γ_1 and γ_2 as a function of the atomic density n.

It is shown in Ref. 26 that precise measurements of γ_1 and γ_2 and of a quantity which is proportional to the atomic density n can be performed. The method is based on the analysis of the modulation of the maser level of oscillation, which is induced by a modulation of the atomic populations in the beam, in appropriate conditions of operation.

As shown in Fig. 1 one then obtains the variation of γ_{1e} and γ_{2e} as a function of the measurable quantity $K_1 Q_c R_0 / T_b$ defined in Ref. 26. One has, in cgs units,

$$K_1 Q_c \frac{R_0}{T_b} = 4\pi \frac{\mu_0^2}{\hbar} \eta \frac{V_b}{V_c} \frac{Q_c}{T_b} (\rho_{22} - \rho_{44})_B n = \alpha n, \tag{4}$$

where η is the filling factor of the cavity, as defined in Refs. 22 and 23; V_b and V_c are the volume of the bulb and the cavity, respectively; μ_0 is the Bohr magneton; h is Planck's constant, and $(\rho_{22} - \rho_{44})_B$ is the population difference between atoms in states $F=1$, $m=0$ and $F=0$, $m=0$ in the beam entering the bulb.

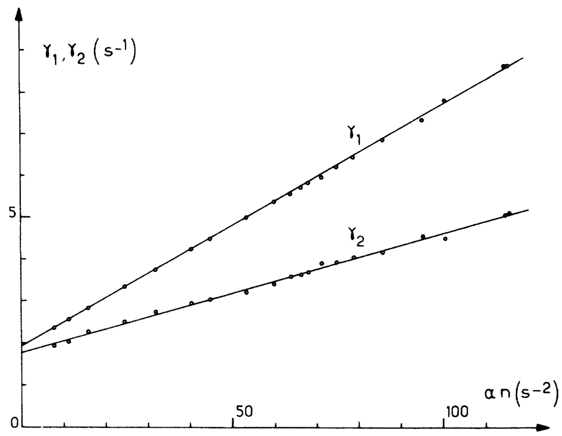

FIG. 1. Variation of the relaxation rates γ_1 and γ_2 as a function of the measurable quantity αn, where α is defined by Eq. (4). In that measurement, the temperature was 253 K.

The measurement of the physical quantities, such as $\eta V_b/V_c$, Q_c, T_b, and $(\rho_{22}-\rho_{44})_B$, which are characteristic of the hydrogen maser used, therefore allows the determination of the absolute value of the density of hydrogen atoms. The values of σ for the considered temperatures result.

EXPERIMENTAL SETUP

Our hydrogen maser has been specifically designed to operate over a very large temperature range. As shown in Fig. 2 the microwave cavity and the storage bulb are surrounded by a thermostat. Helium pressure allows very good thermal contact between the bulb and the thermostat. Control of the helium pressure is used for the fine tuning of the microwave cavity. An evacuated chamber ensures the thermal insulation of the thermostat. All of these parts, which are situated inside a magnetic shield made of three layers of high-magnetic-permeability materials, are made of quartz, Teflon, copper or selected amagnetic copper alloys.

The cryostat is filled with liquid nitrogen for measurement at 77 K. Temperature-regulated liquids are smoothly circulated to stabilize the temperature in the range from 130 to 363 K. Isopentane is used below room temperature and glycol above that temperature. The design allows a temperature homogeneity over the bulb and the microwave cavity of better than 0.1 K. Because of the very large thermal inertia of the device, temperature fluctuations at a given point in the microwave cavity are smaller than 0.01 K for several hours. These achievements are necessary to allow precise measurements to be made.

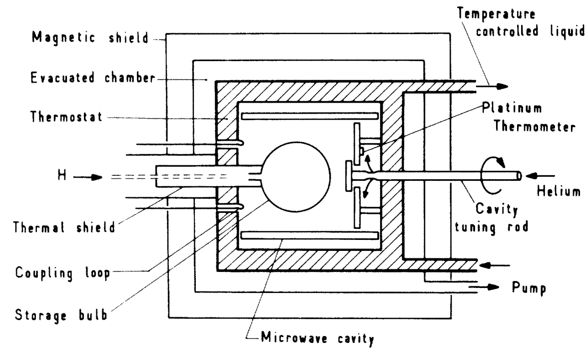

FIG. 2. Schematic diagram of the thermostat which completely surrounds the microwave cavity and the storage bulb of the maser.

The design of the other parts of the maser, including the hydrogen source, the state selector, and two titanium sputtering pumps, is similar[27] to that of masers built for frequency-standard work.

EXPERIMENTAL RESULTS

The computed value of the filling factor $\eta V_b/V_c$ equals 0.385 ± 0.02. For each temperature the cavity quality factor is measured by standard methods, and the value of T_b is deduced from the observation of the buildup of the maser oscillation.[26] The precision in the measurement of Q_c and T_b equals 2% and 3%, respectively.

For the case where the state selection by the hexapole magnet would be perfect, only atoms in states $F=1$, $m=1$ and $F=1$, $m=0$ would enter the bulb, and $(\rho_{22}-\rho_{44})_B$ would be equal to 0.5. However, the beam is contaminated with atoms in states $F=1$, $m=-1$ and $F=0$, $m=0$ and the value of $(\rho_{22}-\rho_{44})_B$ needs to be determined. This can be done as explained below.

Between the magnet and the bulb, the distribution of atoms in states $F=1$, $m=0$ and $F=1$, $m=1$, for which $m_J=\frac{1}{2}$ in the strong field of the hexapole magnet, differs from that of other atoms, for which $m_J=-\frac{1}{2}$ in the magnet, as shown in Fig. 3. In particular, when a beam shutter begins to intercept atoms entering the bulb, only atoms in states $F=1$, $m=0$ and $F=1$, $m=1$ are removed from the beam. It can then be shown[22] that under that condition the fractional variation of the measured quantity αn, defined in Eq. (4), equals

$$\frac{\alpha n-\alpha' n'}{\alpha n}=\frac{1}{2(\rho_{22}-\rho_{44})_B}\,\frac{n-n'}{n}\,, \tag{5}$$

where α' and n' are the values of α and n when the shutter intercepts atoms entering the bulb.

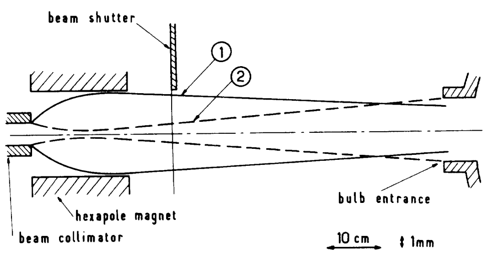

FIG. 3. Schematic diagram of the atomic beam showing the distribution of atoms in the beam cross section. When the beam shutter begins to intercept atoms entering the bulb, it removes atoms in states $F=1$, $m=0$ and $F=1$, $m=1$ only. (1) Envelope of trajectories for atoms in states $F=1$, $m=1$ and $F=1$, $m=0$ which are able to enter in the bulb, for a given velocity. (2) Envelope of trajectories for atoms in states $F=1$, $m=-1$ and $F=0$, $m=0$ which are able to enter in the bulb, for the same velocity.

On the contrary, when the beam intensity is adjusted by varying the pressure in the atomic source, the value of α is not modified and the fractional variation of the measured quantity αn equals the fractional variation of the atomic density n. It is therefore possible to measure the value of $(\rho_{22}-\rho_{44})_B$ by comparing measurements of γ_{1e}, γ_{2e}, and αn made when varying the beam intensity, either by displacing the beam shutter or by varying the pressure in the atomic source. One then obtains $(\rho_{22}-\rho_{44})_B = 0.40 \pm 0.04$.

Figure 4 shows the experimental value of the ratio γ_{1e}/γ_{2e} in the considered range of temperature. It is very close to the theoretical value of 2.[5] This result confirms that the observed density-dependent variation of γ_{1e} and γ_{2e} is characteristic of H-H collisions.

The temperature dependence of the hydrogen-

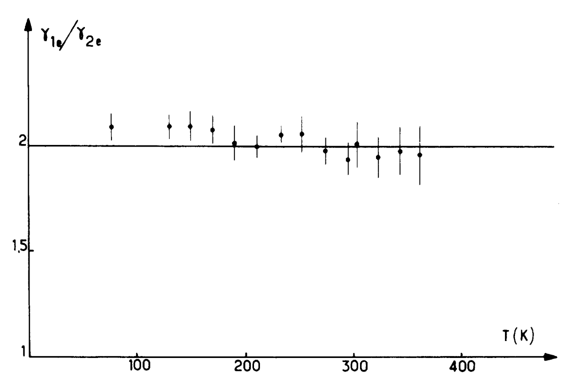

FIG. 4. Experimental values of the ratio γ_{1e}/γ_{2e} in the considered range of temperature. The error bar is given for a confidence interval of 0.90.

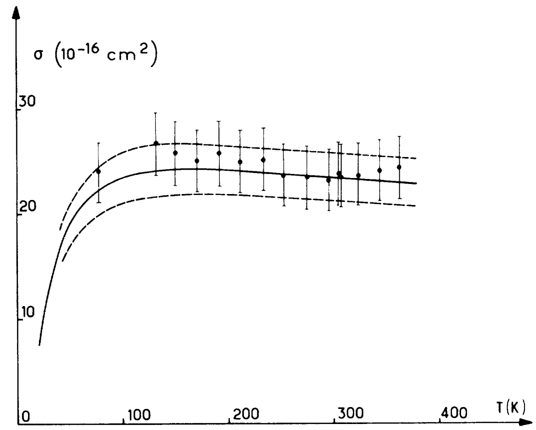

FIG. 5. Temperature dependence of the hydrogen spin cross section σ. The dots with error bars represent the experimental values. The solid line represents the theoretical values calculated by Allison, and the dotted lines specify the 10% uncertainty limit on these theoretical values.

hydrogen spin-exchange cross section is depicted in Fig. 5, where the mean value of the two determinations of σ, obtained from the measurement of the variations of γ_{1e} and γ_{2e} with the atomic density, are plotted. The uncertainty in the determination of $\eta V_b/V_c$ and in the measurement of $(\rho_{22}-\rho_{44})_B$ is included in the error bars, along with the uncertainties in other measurements. It should be noted that uncertainties in the values of $\eta V_b/V_c$ and $(\rho_{22}-\rho_{44})_B$ would not affect a plot of the temperature dependence of σ/σ_0, where σ_0 is the spin-exchange cross section, at some agreed-upon reference temperature, such as room temperature.

The total experimental fractional uncertainty is about 12%. The experimental results vary between 23 and 25.9 Å^2 in the total temperature range and the value for $T=296$ K is $\sigma = 23.1$ Å^2.

These results agree satisfactorily with the theoretical values of $\sigma = (\sigma^+ + \sigma^-)/2$ which are derived from Allison's table for σ^+ and σ^-. The theoretical value of σ for $T=296$ K is $\sigma = 23.5$ Å^2 and there are small variations in the considered temperature range.

In Fig. 5, the solid line represents the temperature dependence of the theoretical values, and the dotted lines specify the 10% uncertainty limits on these theoretical values.

ACKNOWLEDGMENT

We are indebted to Dr. P. Petit for the design and the preparation of the experimental setup.

[1]E. M. Purcell and G. B. Field, Astrophys. J. 124, 542 (1956).
[2]A. Dalgarno, Proc. R. Soc. A 262, 132 (1961).
[3]A. Dalgarno and R. J. W. Henry, Proc. Phys. Soc. (Lond.) 83, 157 (1964).
[4]A. Dalgarno, Rev. Mod. Phys. 39, 850 (1967).
[5]J. P. Wittke and R. H. Dicke, Phys. Rev. 103, 620 (1956).
[6]A. F. Hildebrandt, F. B. Booth, and C. A. Barth, J. Chem. Phys. 31, 273 (1959).
[7]R. M. Mazo, J. Chem. Phys. 34, 169 (1961).
[8]P. L. Bender, Phys. Rev. 132, 2154 (1963).
[9]S. B. Crampton and H. T. M. Wang, Phys. Rev. A 12, 1305 (1975).
[10]S. B. Crampton, Phys. Rev. 158, 57 (1967).
[11]F. J. Smith, Planet. Space Sci. 11, 126 (1963).
[12]A. E. Glassgold and S. A. Lebedeff, Ann. Phys. (N.Y.) 28, 181 (1964).
[13]E. Roueff, C. R. Acad. Sci. B 264, 1713 (1967).
[14]F. Grossetête, J. Phys. (Paris) 25, 383 (1964); 29, 456 (1968).
[15]L. C. Balling, R. J. Hanson, and F. M. Pipkin, Phys. Rev. 133, A607 (1964).
[16]A. C. Allison and A. Dalgarno, Astrophys. J. 158, 423 (1969).
[17]A. C. Allison, Phys. Rev. A 5, 2695 (1972).
[18]W. Kolos and L. Wolniewicz, J. Chem. Phys. 43, 2429 (1965).
[19]H. Hellwig, Phys. Rev. 166, 4 (1968).
[20]C. Audoin, Physics Lett. 28A, 372 (1968).
[21]J. Vanier, R. Brousseau, and R. Larouche, Can. J. Phys. 51, 1901 (1973).
[22]M. Desaintfuscien, Ph.D. thesis (Univ. Paris-Sud, 1975) (CNRS registration No. AO 12310) (unpublished).
[23]D. Kleppner, H. M. Goldenberg, and N. F. Ramsey, Phys. Rev. 126, 603 (1962).
[24]D. Kleppner, H. C. Berg, S. B. Crampton, N. F. Ramsey, R. F. C. Vessot, H. E. Peters, and J. Vanier, Phys. Rev. 138, A972 (1965).
[25]M. Desaintfuscien, P. Petit, C. Audoin, and J. P. Schermann, C. R. Acad. Sci. B 270, 906 (1970).
[26]M. Desaintfuscien and C. Audoin, J. Phys. (Paris) 35, 829 (1974).
[27]P. Petit, J. Viennet, R. Barillet, M. Desaintfuscien, and C. Audoin, Metrologia 10, 61 (1974).